Engineering Science and Technology, an International Journal 21 (2018) 664–671

HOSTED BY

ELSEVIER

Contents lists available at ScienceDirect

Engineering Science and Technology, an International Journal

journal homepage: www.elsevier.com/locate/jestch

Full Length Article

Comparison of DC link current and stator phase current in inverter switching faults detection of PMSM drives in HEVs

Mustafa Aktas [a,*], Hilmi Aygun [b]

[a] Department of Electrical and Electronics Engineering, Ondokuz Mayis University, Samsun, Turkiye
[b] Department of Electrical and Electronics Engineering, Karabuk University, Karabuk, Turkiye

ARTICLE INFO

Article history:
Received 30 March 2018
Revised 22 May 2018
Accepted 3 June 2018
Available online 23 June 2018

Keywords:
Inverter switch fault
DC link current
DWT-based fault diagnosis
Hybrid electric vehicle
Artificial neural network
Field oriented controlled PMSM

ABSTRACT

In this paper, a robust method for detection of inverter short circuit faults in field oriented control (FOC) of permanent magnet synchronous motor (PMSM) drive that is used frequently in hybrid electric vehicles (HEV) thanks to high power density and high efficiency is introduced. In the proposed method, a fault diagnostic and protection technique is developed by using discrete wavelet transform (DWT) and artificial neural network (ANN). The Symlet2 wavelet is selected to perform stator current analysis and the DWT coefficients of the motor currents are used as inputs of ANN for detecting inverter faults in PMSM drives. In HEVs, motor faults can cause permanent damage and accidents. So the early detection of PMSM drive faults in HEV will be provided by the proposed method. For implementing this method, the Matlab program is used to process DWT of signals. DC link and phase currents are compared in inverter switch faults detection and the results show that the proposed technique is very effective for fault diagnostic.

1. Introduction

The permanent magnet synchronous motor (PMSM) is frequently preferred for hybrid electric vehicle (HEV) propulsion thanks to its high power density and high efficiency. In a HEV application, parameters of the PMSM must be selected carefully in order to minimize losses and PMSM must operate at varying loads and speeds. However, electrical losses are minimized by control action in PMSM. The minimization of losses in the PMSM will minimize the current from the dc source [1,2].

In HEV the speed and position control of PMSM drive is required for power management, which determines when internal combustion engine or electric motor will operate, so field oriented control (FOC) which is a kind of vector control, is necessary for HEV. The other important subject is the faults of three phase inverter fed PMSM drive. The most common failures in motor drives are open-circuit faults and short-circuit faults in the inverter. If an open circuit fault happens in an IGBT switch, unstable oscillation occurs [3]. Also if there is a short circuit fault in an IGBT switch, the short circuit current signals exhibit more fluctuation than open circuit current signals. Between these faults, the most serious one is short circuit faults for PMSM drives in HEVs. Because current through IGBT increases rapidly until it saturates and also the gate signal of other switch in the same inverter leg must be turned off immediately because of connection to the DC bus so the IGBT can be destroyed and cause catastrophic failures and permanent magnet can weak if this fault is not continuously monitored and detected early [4–6]. So condition monitoring and the early detection of these faults for PMSM drives in HEVs are very important for protection, control, safety and cost-effective maintenance. By diagnosing the electric motor faults quickly, the life cycle of the electric motor in HEV can be extended [7–9].

Operating conditions of the IGBT switches used in the inverter circuit vary widely so they increase complexity of fault detection and diagnose system for PMSM drives in HEV. For this reason, detecting the faults in inverter fed AC drives has become a research topic. One of these methods is based on artificial intelligence (AI) which is not appropriate for real time analysis with its complex structure. The other developed method is based on comparison of actual and reference voltages by using extra sensors so it increases costs and complexity of the system. The standard digital signal processing based techniques such as discrete Fourier transform (DFT), fast Fourier transform (FFT) are used for condition monitoring and fault diagnostic of motors but these techniques can be implemented separately in time and frequency domains. In the standard digital signal processing techniques, fault currents

* Corresponding author.
E-mail address: mustafa.aktas@omu.edu.tr (M. Aktas).
Peer review under responsibility of Karabuk University.

https://doi.org/10.1016/j.jestch.2018.06.002
2215-0986/

are often non-periodic and non-stationary so performance of these techniques is limited according to the constraint on the window size. Therefore, the advanced digital signal processing based techniques such as discrete wavelet transform (DWT) is required. Because they can be applied together in time and frequency domains which extend the window size [9–14]. Sometimes according to the DWT coefficients, more than one switches in the inverter can appear faulty although one of them is faulty. So this problem can be solved by artificial neural network (ANN) since it is very efficient in the field of classification. The potential benefits of ANN extend beyond the high computation rates provided by massive parallelism of the networks. In additionally, adaptation and continuous learning are parts of an ANN. These properties are very important for nonlinear processes. Therefore, ANN is required for discriminating the healthy switches from the others.

In this study, a robust method is developed to ensure high reliability for detecting short circuit faults by using DWT and ANN. DWT the six level wavelet packet transformed coefficients of both DC link current and stator phase currents are used as inputs of ANN for detecting the failure switch which causes short circuit fault. ANN is used to classify the results. Monitoring the stator current signal of inverter fed PMSM drives is enough for protection purposes. Any other sensors are not required in the proposed PMSM drive for fault diagnosis and this is one of the most used methods for applications.

In the most of the studies, either DC link current or stator phase currents were investigated but in this study both of them are analyzed and compared with each other. The results demonstrate that the proposed method has great capabilities. Also the analyses of DC link current and stator phase currents show that they have some advantages against each other's.

2. Field oriented control of PMSM in hybrid electric vehicles

Nowadays PMSMs are frequently used in HEVs thanks to their structure, high efficiency and robustness. In recent years torque ripples and harmonics in PMSM have been tried to reduce. There are two popular ways for inverter control. One of them is voltage control such as space vector modulation and the other one is current control such as hysteresis and delta modulation [15,16]. Since important improvements have been made regarding the control techniques, especially the FOC with its flux/torque decoupling feature has no better alternative in PMSM drives. FOC which is preferred instead of scalar control especially in high speed range, is one of the vector control methods. The goal of FOC is to control torque variations demand in HEVs and mechanical speed. Also the aim of FOC is to regulate stator phase currents in order to prevent current spikes during transient phases [17,18]. In HEVs when both position and speed control are required for power management, vector control by DSP is implemented. The FOC is implemented successfully in order to force the motor to track the command trajectory in spite of motor load variations [19]. In this control method, stator phase currents are controlled in synchronous *d-q* frame in order to reduce torque ripple for quieter motor operation.

In FOC, two phase equivalent circuit in *d-q* frame and α–β frame are used instead of three phase circuit in order to analyze PMSM drives easily. For this purpose, *abc* to $\alpha\beta$ (Clarke) and $\alpha\beta$ to *dq* (Park) transformations are used widely. FOC block diagram of PMSM drives in HEV is shown in the Fig. 1. In this control method, while *d*-axis stator current controls flux linkage directly, *q*-axis stator current controls torque. For controlling the current, flux and torque, a compact and reliable motor model is required. The AC motor analysis techniques can also be used for PMSM in high performance electric vehicles [20]. Mathematical model of the PMSM with the electrical and mechanical equations in *d-q* frame is given as follows [21,22]:

$$\frac{di_d}{dt} = \frac{1}{L_d}(V_d - R_s i_d + \omega_r L_q i_q) \tag{1}$$

$$\frac{di_q}{dt} = \frac{1}{L_q}[V_q - r_s i_q - \omega_r(L_d i_d + \Psi_m)] \tag{2}$$

$$\psi_d = L_d i_d + \psi_m \tag{3}$$

$$\psi_q = L_q i_q \tag{4}$$

$$\frac{d\omega_{rm}}{dt} = \frac{1}{J}(T_e - T_L - B\omega_{rm}) \tag{5}$$

$$\omega_r = \frac{p}{2}\omega_{rm} \tag{6}$$

$$\frac{d\theta_r}{dt} = \omega_r \tag{7}$$

The electromagnetic torque T_e is given by:

$$T_e = \frac{3}{2}p[\Psi_m i_q + (L_d - L_q) i_d i_q] \tag{8}$$

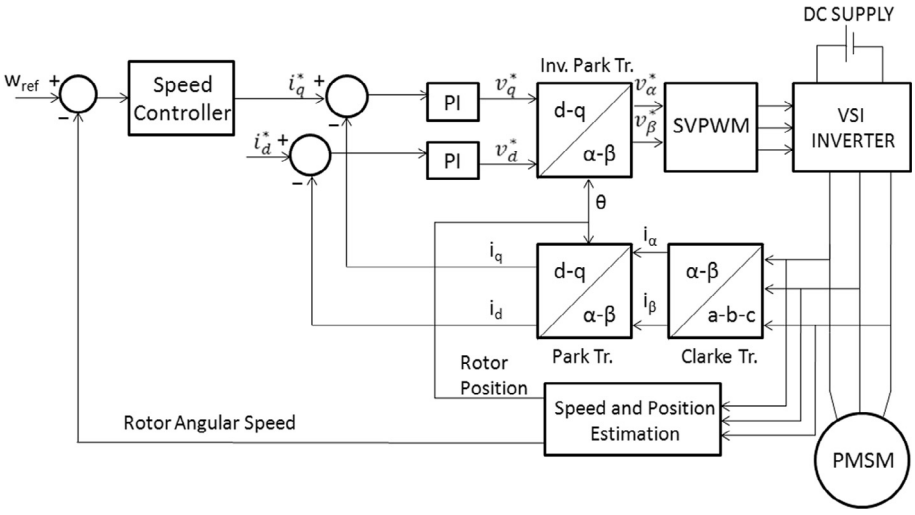

Fig. 1. FOC block diagram of PMSM in HEVs.

where V_d and V_q are d-q axis voltages, i_d and i_q are d-q axis stator currents, L_d and L_q are d-q axis inductances, R_s is stator resistor, Ψ_m is permanent magnet flux, ω_r is electrical angular speed of the rotor, ω_{rm} is mechanical speed of the rotor, Ψ_d and Ψ_q are d-q axis flux linkages, J is inertial torque, T_L is load torque, B is viscous friction coefficient, p is pole number and θ_r is rotor position.

In the third equation, if $i_d = 0$, d axis flux linkage Ψ_d is constant. Since the permanent magnet flux Ψ_m is constant in PMSM drives, the electromagnetic torque which is given by the follow equation is proportional to the q axis current i_q [19].

$$T_e = \frac{3}{2} p \Psi_m i_q \tag{9}$$

Fig. 2 shows the general block diagram of HEV which is simulated.

2.1. Wavelet analysis

The Wavelet Transform (WT) analyses a given signal by convolution with a set of basic functions. These basis functions or wavelet functions are obtained from a mother wavelet by scaling and shifting operations [23]. A wavelet is a small localized wave of particular shape and finite duration that has an average value of zero. The advantage of the WT is its band which can be fine adjusted. In this manner, high and low frequency components can be detected separately and precisely. Results of wavelet transform can be shown on both time and frequency domains [24]. Wavelet is a waveform of limited duration and tends to be irregular, asymmetric, short and oscillatory waveforms. Different wavelet techniques are used depending on the problems that need to be assessed [23].

The main advantage of WT over short time-Fourier transform (STFT) is that the size of analysis window varies in proportion to the frequency. Fourier techniques cannot simultaneously achieve good localization in both time and frequency for a signal. Power signals generally include a combination of transients and harmonics, for which STFT and other conventional time–frequency methods are less suited for analysis. Consequently, WT can be chosen for a better compromise in terms of localization. Wavelet analysis can use more window function in all frequency components, or achieves linear resolution in the whole frequency domain which is weak points of Fourier analysis. As a result, wavelet transform is more preferable in time frequency analyses [15].

DWT can extract the features of current signals for improving an efficient fault detection system. It is a promising method to capture signs of current fault conditions with its frequency and time information. Let us consider $C_0[n]$ as the original signal sequence. After the convolution with h and g quadrature mirror filters, $C_0[n]$ can be decomposed into approximation component $C_1[n]$ and detail component $d_1[n]$ at the first level of decomposition. $C_1[n]$ can be further decomposed into $C_2[n]$ and $d_2[n]$ at the next level of decomposition and this decomposition can go on like that. The components at the end of decomposition are obtained at below [25].

$$C_m[n] = \sum_k h[k-2n] C_{m-1}[k] \tag{10}$$

$$d_m[n] = \sum_k g[k-2n] C_{m-1}[k] \tag{11}$$

where m, n and k represent the level of decomposition, sampling points and translation coefficients, respectively.

In the proposed method, the 6th level of decomposition is used and the Symlet2 wavelet is performed to analyze three phase

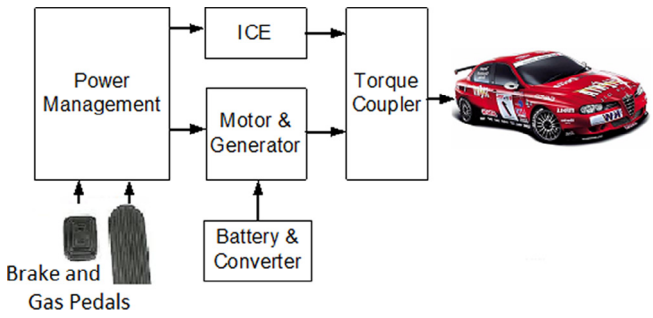

Fig. 2. General block diagram of HEV.

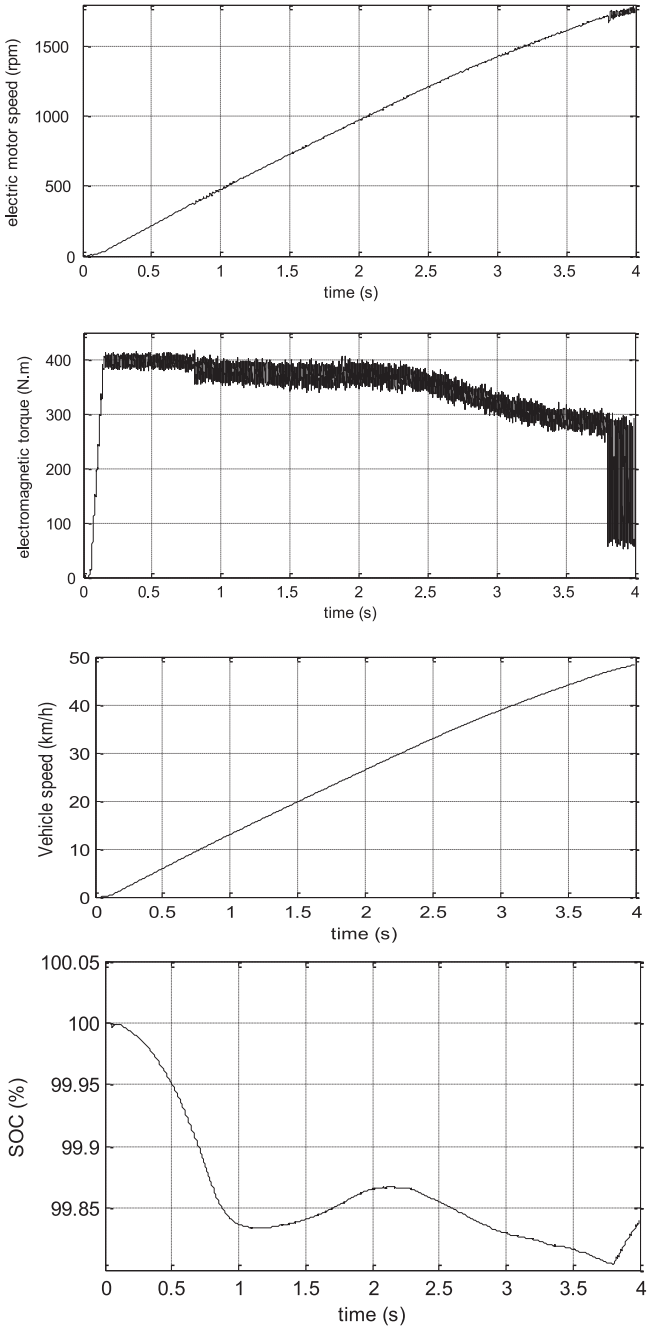

Fig. 3. Faulty operation signals of PMSM drive in HEV, electromagnetic torque, motor speed, vehicle speed and SOC.

stator currents and DC link current. DWT is applied to extract various features from the current patterns, such as the mean energy value for each detail signal. These values are used to detect the short circuit fault and identify the faulty switch. Also ANN is used to classify the mean energy error values in order to identify the faulty switch according to the trained data.

2.2. Artificial neural network (ANN)

ANN is a real simulation of a nervous system and is very efficient in the field of classification. Determination of number of hidden layers and neurons in each layer is one of the most important problems in the studies of neural architecture. Training of an ANN with a lot of neurons takes more time than an ANN with less neuron. However, the ANN with less neuron can have high errors and prevent the training process [20,23,26].

The errors of the network output are used to adjust the weight coefficients of the layers thanks to the back propagation [27]. The ANN has the ability to produce new (previously unseen) data from the training data. It is needed to calculate the derivative of the error with respect to the weight in order to update the weight [28]. The following equations show the relations among inputs, activity level and output:

$$a = W^T I \tag{12}$$

$$o_{hidden} = \log sig(J) \tag{13}$$

$$o_{output} = purelin(a) \tag{14}$$

where W and I are weights and input vectors of the neuron, a is activity level of the neuron, J is the input vector for the neurons of hidden layers and o is the output of the neuron, respectively. The error e can be calculated from the equation at below:

$$e = \frac{1}{2}(d-o)^2 \tag{15}$$

$$\Delta w_j = -\eta(d-o)f'(a)I_j j = 0,1,2,\ldots,n \tag{16}$$

where d is the desired value of the output, the learning factorη is a positive constant. Therefore the weight coefficients of the network can be updated as follows:

$$w_j(new) = w_j(old) + \Delta w_j j = 0,1,2,\ldots,n \tag{17}$$

2.3. Proposed fault detection system in field oriented control of PMSM in HEV

The Matlab/SIMULINK program was used to perform a FOC simulation of PMSM drive in HEV [9], and DWT of the resulting signals by using ANN. The faulty operation signals of electromagnetic torque, electric motor speed are shown in Fig. 3. Also the speed of HEV and state of charge (SOC) are given in the same figure.

When a short circuit fault occurs in driver using IGBTs, stator currents and DC link current show unstable oscillation, as shown in Fig. 4. In this simulation, a short circuit fault in IGBT 1 occurs at 3.8 s and as a result currents in all phases and DC link current are affected.

In this study, wavelet decomposition by using the Symlet2 wavelet is performed on three phase stator currents and DC link current, as shown in Fig. 5. The variations in decomposition coefficients of stator phase currents and DC link current include important information for detecting the faulty switch. Also the sharp variation of signal can be regarded as an indication of the short circuit fault.

In time domain analysis, the faulty power switch can be easily discriminated from the healthy ones by using ANN. In fact, detailed levels, such as e_{a6}, e_{d5}, e_{d6} and e_E are distinguishable between the decomposition coefficients of wavelet analysis.

In Tables 1–4, mean energy values for three phase stator currents and DC link current using symlet2 wavelets at a six level decomposition are shown for the different short circuit fault scenarios. These values enable us to differentiate between the no-fault and faulty conditions. e_{a6}, e_{d5}, e_{d6} and e_E values are used as inputs of ANN and the faulty power switch can be distinguished.

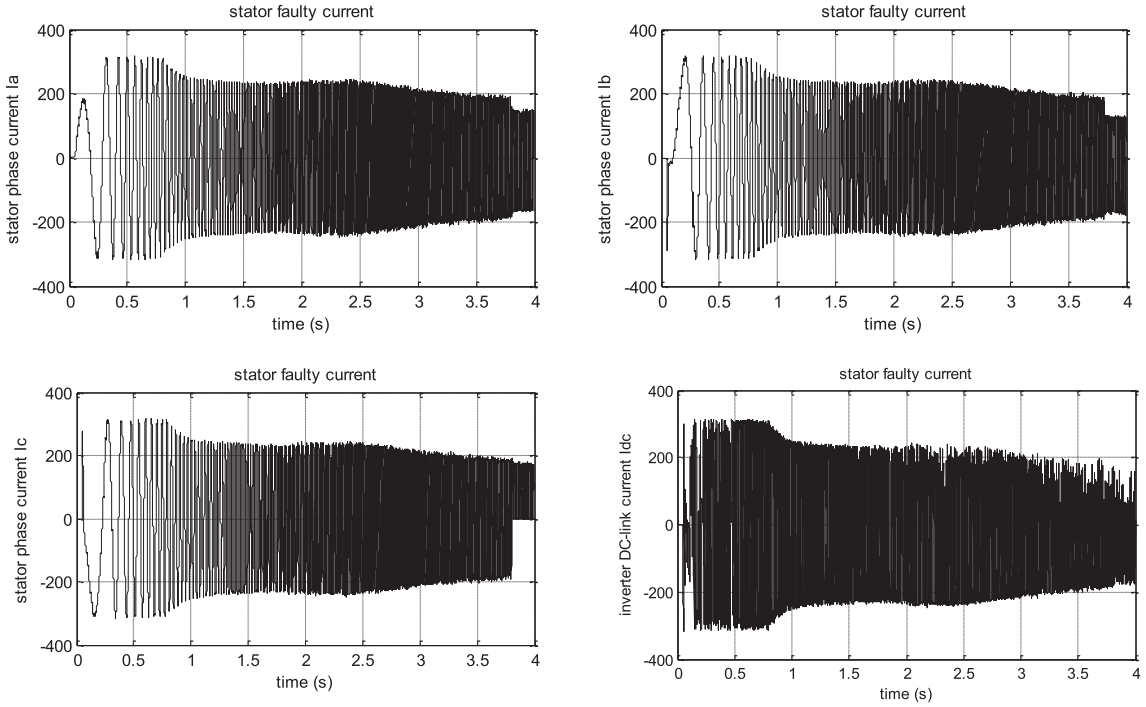

Fig. 4. Stator phase currents and DC link current for IGBT 1 short circuit fault.

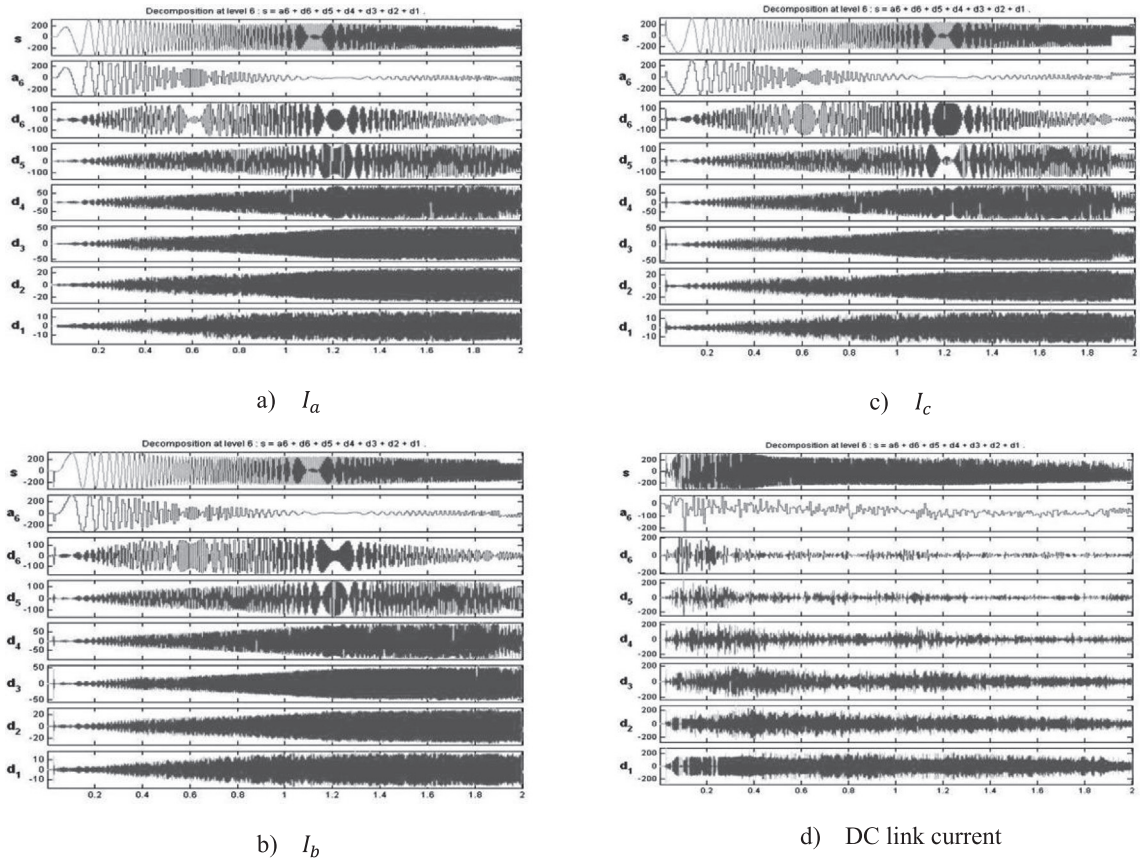

Fig. 5. Symlet2 wavelet level six decomposition of stator currents.

Table 1
I_a stator phase current DWT mean energy values.

	a_6	d_1	d_2	d_3	d_4	d_5	d_6	E
NO FAULT	38,4992	0,0189	0,0386	0,3839	4,6127	26,3761	30,0706	10,2501
IGBT1	38,9044	0,0191	0,0406	0,3895	4,5305	26,8345	29,2813	10,1826
IGBT2	41,1799	0,0177	0,0363	0,3618	4,2556	25,5260	28,6227	9,8034
IGBT3	38,8172	0,0186	0,0402	0,4002	4,5174	25,6198	30,5864	10,1971
IGBT4	39,8002	0,0178	0,0369	0,3710	4,3236	25,0265	30,4241	10,0333
IGBT5	39,2728	0,0187	0,0399	0,3868	4,3663	25,0786	30,8369	10,1212
IGBT6	45,1996	0,0164	0,0337	0,3302	3,8951	22,9687	27,5564	9,1334

Table 2
I_b stator phase current DWT mean energy values.

	a_6	d_1	d_2	d_3	d_4	d_5	d_6	E
NO FAULT	39,8267	0,0189	0,0384	0,3809	4,5881	25,0383	30,1087	10,0289
IGBT1	39,9736	0,0183	0,0397	0,3956	4,4774	24,2177	30,8776	10,0044
IGBT2	41,0389	0,0174	0,0361	0,3640	4,2667	23,6520	30,6249	9,8269
IGBT3	41,1770	0,0186	0,0393	0,3822	4,3217	24,0075	30,0538	9,8038
IGBT4	46,2601	0,0162	0,0331	0,3357	3,9392	22,0772	27,3384	8,9566
IGBT5	40,4381	0,0188	0,0402	0,3895	4,4817	24,7831	29,8487	9,9270
IGBT6	42,1588	0,0176	0,0361	0,3518	4,1959	23,4567	29,7832	9,6402

Stator dc offset current polarity and DC link offset current polarity is checked to detect the faulty switches in three phase inverter circuit. Tables 5 and 6 are the fault decision tables. But the tables which include the error coefficients are not enough to find the faulty switch. So an ANN that is trained by using the error coefficients is used to find the faulty switch.

Table 3
I_c stator phase current DWT mean energy values.

	a_6	d_1	d_2	d_3	d_4	d_5	d_6	E
NO FAULT	42,5510	0,0185	0,0375	0,3730	4,5008	27,1967	25,3225	9,5748
IGBT1	43,5775	0,0181	0,0392	0,3771	4,2388	25,7273	26,0220	9,4037
IGBT2	48,1319	0,0159	0,0332	0,3321	3,8932	23,7761	23,8176	8,6447
IGBT3	42,9864	0,0182	0,0399	0,3774	4,3773	26,7943	25,4066	9,5023
IGBT4	45,4657	0,0167	0,0354	0,3460	4,0658	25,3637	24,7067	9,0890
IGBT5	43,3292	0,0181	0,0401	0,3851	4,3411	26,4725	25,4139	9,4451
IGBT6	44,5811	0,0173	0,0355	0,3467	4,1279	25,6977	25,1939	9,2365

Table 4
DC link current DWT mean energy values.

	a_6	d_1	d_2	d_3	d_4	d_5	d_6	E
NO FAULT	17,7980	17,4253	17,0498	17,0118	14,4975	9,4750	6,7427	13,7003
IGBT1	17,3177	17,2952	16,9760	17,1305	14,6918	9,7634	6,8254	13,7804
IGBT2	30,2509	14,9074	14,8120	14,3059	12,2216	7,8961	5,6062	11,6249
IGBT3	17,2322	17,3367	16,9960	17,1587	14,6983	9,7749	6,8032	13,7946
IGBT4	34,5771	14,3350	14,1995	14,2236	10,6162	6,6476	3,8572	10,9038
IGBT5	20,2928	17,1272	16,7262	17,8094	14,0500	9,0042	4,9903	13,2845
IGBT6	29,7912	14,8465	14,8474	15,0334	12,0529	7,8060	5,6225	11,7015

Table 5
I_a stator phase current DWT mean energy error values

	e_{a6}	e_{d1}	e_{d2}	e_{d3}	e_{d4}	e_{d5}	e_{d6}	e_E
IGBT1	−0,4052	−0,0002	−0,0020	−0,0056	0,0822	−0,4584	0,7893	0,0675
IGBT2	−2,6807	0,0012	0,0023	0,0221	0,3571	0,8501	1,4479	0,4467
IGBT3	−0,3180	0,0003	−0,0016	−0,0163	0,0953	0,7563	−0,5158	0,0530
IGBT4	−1,3010	0,0011	0,0017	0,0129	0,2891	1,3496	−0,3535	0,2168
IGBT5	−0,7736	0,0002	−0,0013	−0,0029	0,2464	1,2975	−0,7663	0,1289
IGBT6	−6,7004	0,0025	0,0049	0,0537	0,7176	3,4074	2,5142	1,1167

Table 6
DC link current DWT mean energy error values

	e_{a6}	e_{d1}	e_{d2}	e_{d3}	e_{d4}	e_{d5}	e_{d6}	e_E
IGBT1	0,4803	0,1301	0,0738	−0,1187	−0,1943	−0,2884	−0,0827	−0,0801
IGBT2	−12,4529	2,5179	2,2378	2,7059	2,2759	1,5789	1,1365	2,0754
IGBT3	0,5658	0,0886	0,0538	−0,1469	−0,2008	−0,2999	−0,0605	−0,0943
IGBT4	−16,7791	3,0903	2,8503	2,7882	3,8813	2,8274	2,8855	2,7965
IGBT5	−2,4948	0,2981	0,3236	−0,7976	0,4475	0,4708	1,7524	0,4158
IGBT6	−11,9932	2,5788	2,2024	1,9784	2,4446	1,6690	1,1202	1,9988

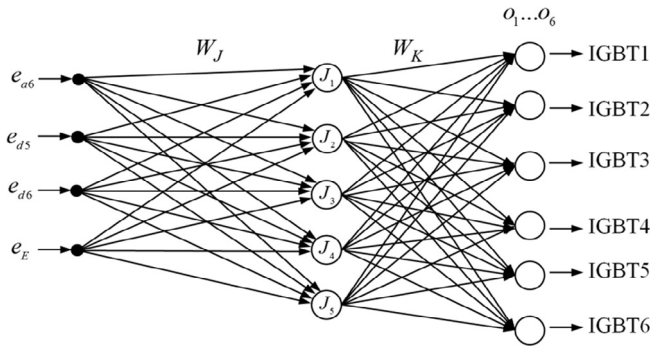

Fig. 6. The proposed ANN estimate system.

For this purpose, we used an ANN which has four inputs and six outputs. The ANN estimate system is proposed to find faulty inverter switch by using DWT coefficients and their errors. The elements of $[W_j]_{4\times5}$ and $[W_k]_{5\times6}$ weight matrix are chosen from −1 to +1 randomly and these weight coefficients are used for hidden layer and output layer. Logarithmic sigmoid activation function and purelin function are chosen for the hidden layer and output layer for each node, respectively. The proposed ANN estimate system is shown in Fig. 6.

As shown in Fig. 7, the faulty switch (IGBT1) is found by using the proposed ANN system for the stator phase current and DC link current. (output1 of IGBT1 is equal to 1 and the other outputs are equal to 0)

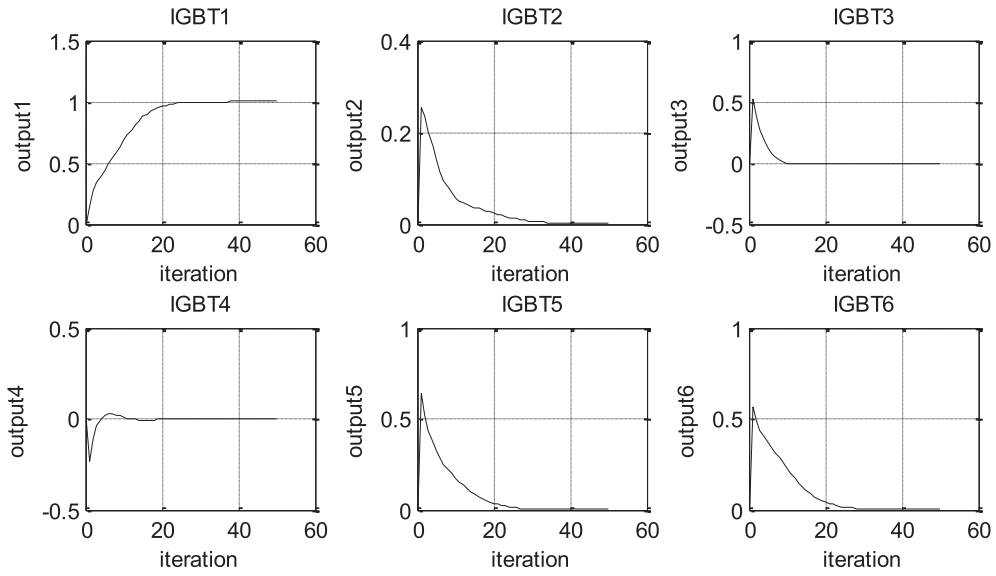

a) For the stator phase current

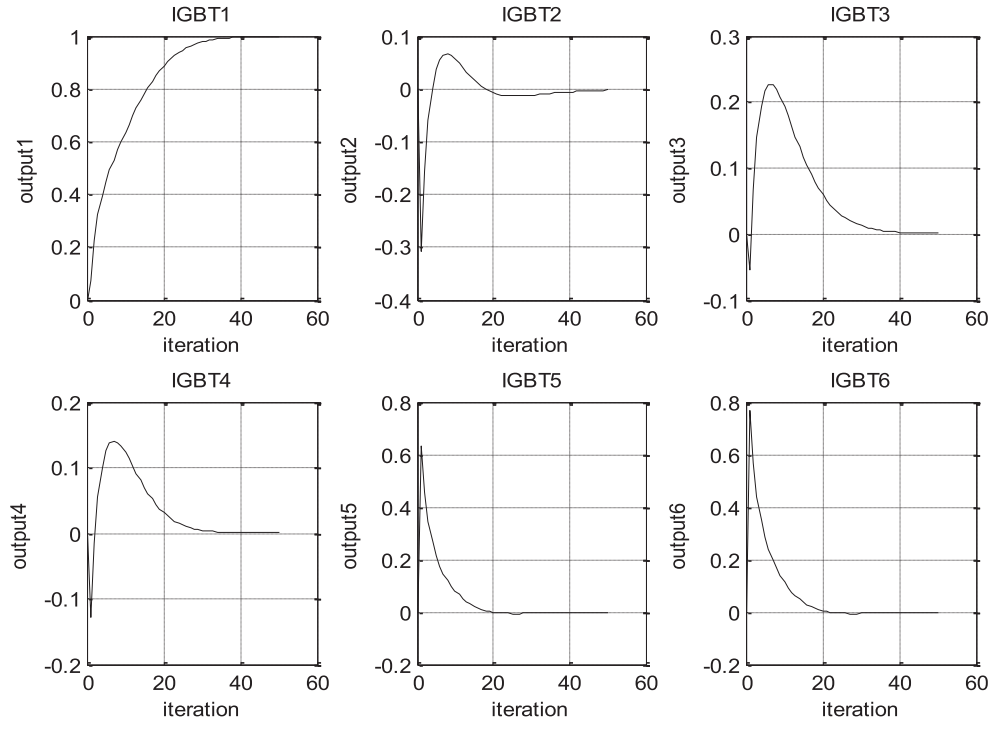

b) For DC link current

Fig. 7. Faulty inverter switch decision using ANN evaluation system.

3. Conclusion

In this paper, the analysis of phase current transients and DC Link current transients during the short-circuit fault in a three phase inverter of PMSM in HEV are realized by using DWT and ANN for classifying. The proposed method can detect the faulty switch easily if a short circuit fault happens. It is known that the DC link current carries the phase current transients. The results show that both of phase current and DC link current have a good capability to find the faulty switch or switches. But in practice, a DC link current sensor will be an extra cost if the phase current sensors are used for control. However the cost will reduce when the DC link current is used for analyses since it requires only one sensor. Setting up the hardware is under consideration as a future research plan.

Appendix A

Parameters of the Vehicle parameters	
Vehicle model parameters	Rated Value
Vehicle mass	1325 kg
Horizontal distance from center to rear axle	1.6 m
Horizontal distance from center to front axle	1.4 m
Center of gravity height from ground	0.5 m
Frontal area	2.57 m^2
Drag coefficient	0.4
Parameters of the PMSM	
Parameter	Rated Value
Motor power	50 kW
Number of pole pairs	4
Stator resistance	6.5 mΩ
q-axis inductance	2.05 mH
d-axis inductance	1.6 mH
Magnetic flux linkage	0.175 Wb
Inertia	0.089 kg-m^2
Frictional coefficient	0.005 N-m.s

References

[1] M. Hall, J.C. Balda, Permanent Magnet Synchronous Motor Drive for HEV Propulsion: Optimum Speed Ratio and Parameter Determination, Vehicular Technology Conference, Panama, 2002, pp. 1500–1504.

[2] T. Finken, M. Hafner, M. Felden, K. Hameyer, Design rules for energy efficient interior permanent magnet synchronous motors in hybrid electric vehicle applications, Electromotion 17 (3) (2010) 143–154.

[3] M. Aktas, V. Turkmenoglu, Wavelet-based switching faults detection in direct torque control induction motor drives IET Science, Measure. Technol. 4 (6) (2009) 303–310.

[4] J. Hang, S. Ding, J. Zhang, M. Cheng, W. Chen, Q. Wang, Detection of interturn short-circuit fault for PMSM with simple fault indicator, IEEE Trans. Energy Conv. 31 (4) (2016) 1697–1699.

[5] M.A. Mazzoletti, G.R. Bossio, C.H.D. Angelo, D.R. Espinoza-Trejo, A model-based strategy for interturn short-circuit fault diagnosis in PMSM, IEEE Trans. Indust. Electr. 64 (9) (2017) 7218–7228.

[6] C. Chuang, Z. Wei, W. Zhifu, L. Zhi, The diagnosis method of stator winding faults in PMSMs based on SOM neural networks, Energy Procedia 105 (2017) 2295–2301.

[7] B. Akin, S.B. Ozturk, H.A. Toliyat, M. Rayner, DSP-based sensorless electric motor fault diagnosis tools for electric and hybrid electric vehicle powertrain applications, IEEE Trans. Vehicular Technol. 58 (6) (2009) 2679–2688.

[8] H. Aouzellag, K. Ghedamsi, D. Aouzellag, Energy management and fault tolerant control strategies for fuel cell/ultra-capacitor hybrid electric vehicles to enhance autonomy, efficiency and life time of the fuel cell system, Int. J. Hydrogen Energy 40 (2015) 7204–7213.

[9] M. Aktas, A novel method for inverter faults detection and diagnosis in pmsm drives of hevs based on discrete wavelet transform, Adv. Elect. Comput . Eng. 12 (4) (2012) 33–38, https://doi.org/10.4316/AECE.2012.04005.

[10] S. Padmanaban, J.L.F. Febin Daya, F. Blaabjerg, N. Mir-Nasiri, A.H. Ertas, Numerical implementation of wavelet and fuzzy transform IFOC for three-phase induction motor, Eng. Sci. Technol. Int. J. 19 (1) (2016) 96–100, https://doi.org/10.1016/j.jestch.2015.07.002. ISSN: 2215–0986.

[11] S. Padmanaban, F.J.L. Daya, F. Blaabjerg, P.W. Wheeler, P. Szcześniak, V. Oleschuk, A.H. Ertas, Wavelet-fuzzy speed indirect field oriented controller for three-phase AC motor drive – Investigation and implementation, Eng. Sci. Technol. Int. J. 19 (3) (2016) 1099–1107, https://doi.org/10.1016/j.jestch.2015.11.007. ISSN 2215-0986.

[12] Sung-Guk Ahn, Byoung-Gun Park, Rae-Young Kim, Dong-Seok Hyun, Fault Diagnosis for Open-Phase Faults of Permanent Magnet Synchronous Motor Drives using Extended Kalman Filter, 36th Annual Conference on IEEE Industrial Electronics Society, Glendale, 2010, pp. 835–840.

[13] F. Zidani, D. Diallo, M. Benbouzid, R. Nait-Said, A fuzzy-based approach for the diagnosis of fault modes in a voltage-fed PWM inverter induction motor drive, IEEE Trans. Indust. Electr. 55 (2) (2008) 586–593.

[14] R.L.A. Ribeiro, C.B. Jacobina, E.R.C. Silva, A.M.N. Lima, Fault detection of open-switch damage in voltage-fed PWM motor drive systems, IEEE Trans. Power Electr. 18 (2) (2003) 587–593.

[15] A.I.L. Sánchez, E.R. Cadaval, M. Montero, J.G. Lozano, Optimization of losses in permanent magnet synchronous motors for electric vehicle application, in: Doctoral Conference on Computing, Electrical and Industrial Systems, Springer, Caparica, Portugal, 2011, pp. 502–509.

[16] X. Chen, J. Hu, K. Chen, Z. Peng, Modeling of electromagnetic torque considering saturation and magnetic field harmonics in permanent magnet synchronous motor for HEV, Simulation Modell. Practice Theory 66 (2016) 212–225.

[17] M.B.B. Sharifian, T. Herizchi, K.G. Firouzjah, Field oriented control of permanent magnet synchronous motor using predictive space vector modulation, IEEE Symposium on Industrial Electronics and Applications, Kuala Lumpur, 2009, pp. 574–579.

[18] J. Jacob, A. Chitra, Field oriented control of space vector modulated multilevel inverter fed PMSM drive, Energy Procedia 117 (2017) 966–973.

[19] M.S. Merzoug, F. Naceri, Comparison of field-oriented control and direct torque control for permanent magnet synchronous motor (PMSM), Eng. Technol. World Acad. Sci. (2008) 299–304.

[20] C.C. Chan, K.T. Chau, An overview of power electronics in electric vehicles, IEEE Trans. Indust. Electr. 44 (1) (1997) 3–13.

[21] H. Lesani, A. Darabi, Gheidari Z. Nasiri, F. Tootoonchian, Very fast field oriented control for permanent magnet hysteresis synchronous motor, Iranian J. Electrical Electronic Eng. 2 (1) (2006) 34–40.

[22] J. Lara, J. Xu, A. Chandra, Effects of rotor position error in the performance of field-oriented-controlled PMSM drives for electric vehicle traction applications, IEEE Trans. Indust. Electr. 63 (8) (2016) 4738–4751.

[23] S.A. Shaaban, Hiyama Takashi, Discrete Wavelet and Neural Network for Transmission Line Fault Classification, International Conference on Computer Technology and Development (ICCTD 2010), Cairo, 2010, pp. 446–450.

[24] C. Pothisarn, A. Ngaopitakkul, Discrete Wavelet Transform and Back-propagation Neural Networks, Algorithm for Fault Classification on Transmission Line, Transmission & Distribution Conference & Exposition, Thailand, 2009, pp. 1–4.

[25] A. Rohan, S.H. Kim, Fault detection and diagnosis system for a three-phase inverter using a DWT based artificial neural network, Int. J. Fuzzy Logic Intell. Syst. 16 (4) (2016) 238–245.

[26] Y. Nyanteh, C. Edrington, S. Srivastava, D. Cartes, Application of artificial intelligence to real-time fault detection in permanent-magnet synchronous machines, IEEE Indust. Appl. Soc. 49 (3) (2013) 1205–1214.

[27] M. Aktas, H.I. Okumus, Neural Network Based Stator Resistance Estimation in Direct Torque Control of Induction Motor, in: IJCI Proceedings of Intl. XII, Turkish Symposium on Artificial Intelligence and Neural Networks, Turkey, 2003, pp. 355–358.

[28] Yansong Wang, Yanfeng Xing, Hui He, "An Intelligent Approach for Engine Fault Diagnosis Based on Wavelet Pre-processing Neural Network Model", Proceedings of the 2010 IEEE International Conference on Information and Automation, Shanghai, China, 2010, pp. 576–581.